Phase Diagram and Electrical Conductivity of the $PrBr_3$-CsBr Binary System

Leszek Rycerz[a], Ewa Ingier-Stocka[a], Madjid Berkani[b], and Marcelle Gaune-Escard[c]

[a] Chemical Metallurgy Group, Faculty of Chemistry, Wroclaw University of Technology,
Wybrzeze Wyspianskiego 27, 50-370 Wroclaw, Poland
[b] Laboratoire de Génie de l'Environnement, Département de Chimie, Faculté des Sciences Exactes,
Université A. Mira – Béjaïa 06000, Algérie
[c] Ecole Polytechnique, IUSTI CNRS UMR 6595, Technopole de Chateau-Gombert,
5 rue Enrico Fermi,13453 Marseille Cedex 13, France

Reprint requests to M. G.-E.; E-mail: Marcelle.Gaune-Escard@polytech.univ-mrs.fr

Z. Naturforsch. **65a,** 859 – 864 (2010); received October 27, 2009

Phase equilibrium in the $PrBr_3$-CsBr binary system was established from Differential Scanning Calorimetry (DSC). This system has two compounds, Cs_3PrBr_6 and $CsPr_2Br_7$, and three eutectics located at molar fraction of $PrBr_3$ ($x = 0.108$; 850 K), ($x = 0.453$; 767 K), and ($x = 0.757$, 870 K), respectively. Cs_3PrBr_6 undergoes a solid-solid phase transition at 726 K and melts congruently at 1051 K. $CsPr_2Br_7$ undergoes a solid-solid phase transition at 835 K, and melts congruently at 896 K. The electrical conductivity of $PrBr_3$-CsBr liquid mixtures was measured down to temperatures below solidification over the whole composition range. Results obtained are discussed in term of possible complex formation.

Key words: Phase Diagram; Praseodymium Bromide; Cesium Bromide; Electrical Conductivity.

1. Introduction

In spite of their technological importance rare earth halides were poorly characterized until recently. The phase diagrams of the MX-LnX_3 (lanthanide halide-alkali metal halide) binary systems available in literature very often either contain serious errors or lack precision [1]. This situation was the trigger to a systematic investigation program on these systems in order to determine their thermodynamic, structural and electrical conductivity properties, using several complementary experimental techniques. All the lanthanide-alkali metal chloride binary systems have been successfully examined or reexamined by Seifert [2 – 3]. The phase diagrams of the homologous bromide and iodide systems were not fully investigated nor critically assessed yet. Some systems were investigated [4], but the data obtained have been given as a graphic-only information. Moreover, no compositional or temperature values for invariant points were provided by the authors. Therefore it is clear that more details are required to fully characterize those systems. In view of the above discrepancies, or lack of data for many $LnBr_3$-based binary systems, we decided to assess existing data and to investigate the still unexplored lanthanide bromide-based systems. We have found previously that the binary systems of praseodymium(III) bromide with LiBr and NaBr are of simple eutectic-type [1]. The congruently melting compound (K_3PrBr_6) and two incongruently melting compounds (K_2PrBr_5 and KPr_2Br_7) were found in the $PrBr_3$-KBr system [5]. The present work reports the phase equilibria in the $PrBr_3$-CsBr binary system, which are discussed with literature data [6]. In addition the electrical conductivity of $PrBr_3$-CsBr liquid binary mixtures was measured over the whole composition range and a wide temperature range.

2. Experimental

2.1. Chemicals

Praseodymium(III) bromide was synthesised from the praseodymium oxide Pr_6O_{11}. The main steps of this synthesis include, as described previously [1]: dissolution of oxide in hot concentrated HBr acid, crystallisation of $PrBr_3 \cdot nH_2O$, its dehydration in the presence of ammonium bromide, sublimation of NH_4Br, melting of crude $PrBr_3$ and its purification by distillation under reduced pressure (~ 0.1 Pa) in a quartz ampoule at 1150 K. Chemical analysis on $PrBr_3$ was

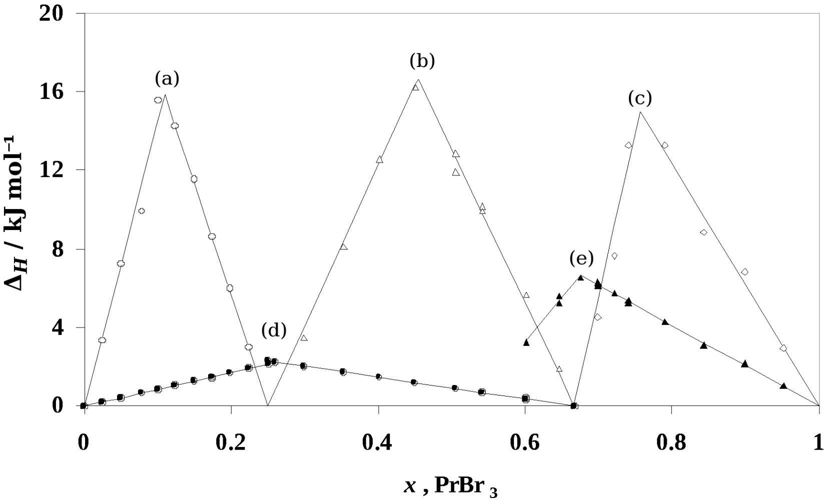

Fig. 1. Tamman constructions for the $PrBr_3$-CsBr system (description in the text).

performed by mercurimetric (bromine) and complexometric (praseodymium) methods. The results were as follows: Pr, 36.96 ± 0.15% (37.02% theoretical); Br, 63.04 ± 0.11% (62.98% theoretical).

Cesium bromide was a Merck Suprapur reagent (minimum 99.9%). Before use, it was progressively heated up to fusion under gaseous HBr atmosphere. Excess HBr was then removed from the melt by argon bubbling.

All chemicals were handled inside a high purity argon atmosphere in a glove box (water content < 2 ppm).

2.2. Measurements

Experimental mixture samples, made from the appropriate amounts of $PrBr_3$ and CsBr, were melted in vacuum-sealed quartz ampoules. The melts were homogenised and solidified. These samples were ground in an agate mortar in a glove box. 34 homogenous mixtures of different compositions were prepared in this way and used in phase diagram and electrical conductivity measurements.

Phase equilibria in the $PrBr_3$-CsBr system were investigated with a Setaram DSC 121 differential scanning calorimeter. Experimental samples (300 – 500 mg) were contained in vacuum-sealed quartz ampoules. Experiments were conducted at heating and cooling rates ranging 1 – 5 K min^{-1}. Details of experimental procedure and apparatus calibration were given previously [1]. The maximum relative experimental error on enthalpy of phase transition did not exceed 1%. Temperature was measured with precision ±1 K.

Electrical conductivity measurements were carried out in the capillary quartz cells described in details elsewhere [7] and calibrated with molten NaCl [8]. The cells constants varied between 10 000 and 12 500 m^{-1}. The change of any individual cell constant was less than 1% after several experiments. The conductivity of the melt was measured by platinum electrodes with the conductivity meter Tacussel CD 810 during increasing and decreasing temperature runs. The mean values of these two runs were used in calculations. Experimental runs were performed at heating and cooling rates 1 K min^{-1}. Temperature was measured with a Pt/Pt-Rh(10) thermocouple with 1 K accuracy. Temperature and conductivity data acquisition was made with PC computer, interfaced to the conductivity meter. All measurements were carried out under static argon atmosphere. The accuracy of measurements was estimated at ±2%.

3. Results

3.1. Phase Diagram

DSC investigations performed on samples with different compositions yielded both the corresponding temperature and enthalpy change occuring in the related sample. Due to the supercooling effect, all temperature and enthalpy values reported here were determined from heating curves. Solidus and liquidus temperatures were determined as T_{onset} and T_{peak} of appropriate effects, respectively.

In all thermograms the endothermic effect observed at the highest temperature corresponds to liquidus.

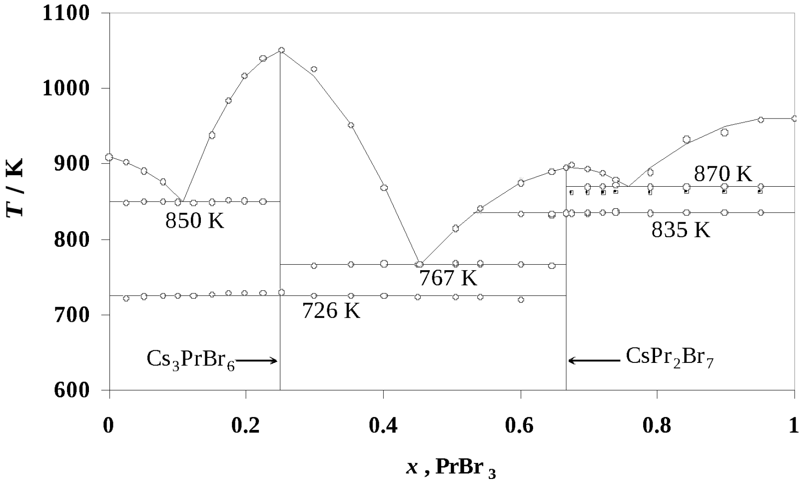

Fig. 2. Phase diagram of the $PrBr_3$-CsBr binary system.

The second endothermic effect, that appears in almost all $PrBr_3$-CsBr mixtures (with the exception of samles with molar fraction of $PrBr_3$, $x = 0.250$ and $x = 0.666$) is dependent on composition. It appears at 850 K, 767 K, and 870 K (mean value from measurements), in the composition ranges $0 < x < 0.250$, $0.250 < x < 0.666$, and $0.666 < x < 1$, respectively. The lack of this effect in the samples of composition $x = 0.250$ and $x = 0.666$ suggests the existence of Cs_3PrBr_6 and $CsPr_2Br_7$ compounds. Indeed, the maximum of temperature on the liquidus curve confirms the existence of these compounds, that melt congruently. Accordingly, the thermal events at 850 K, 767 K, and 870 K correspond to the CsBr-Cs_3PrBr_6, Cs_3PrBr_6-$CsPr_2Br_7$, and $CsPr_2Br_7$-$PrBr_3$ eutectics, respectively.

The eutectics composition was determined accurately from the Tamman plot (Fig. 1a–c). The analysis of this experimental enthalpy vs. composition plot evidences that no solid solutions form in the system. The eutectics composition $x = 0.108 \pm 0.002$, $x = 0.453 \pm 0.010$, and $x = 0.757 \pm 0.017$ was determined from the intercept of the two linear parts in Figure 1a–c, for CsBr-Cs_3PrBr_6, Cs_3PrBr_6-$CsPr_2Br_7$, and $CsPr_2Br_7$-$PrBr_3$ eutectics. The corresponding enthalpy of fusion at the eutectic composition was 15.9 ± 0.6, 16.7 ± 0.7, and 15.0 ± 0.9 kJ mol^{-1}, respectively.

Another thermal effect is observed in samples in the composition range $0 < x \leq 0.666$ at 726 K (mean value for samples of different composition). The Tamman construction for this effect (Fig. 1d) indicates undoubtedly that it is related to the Cs_3PrBr_6 compound. The molar enthalpy associated to this effect (calculated for the Cs_3PrBr_6 compound), $\Delta H_m = 8.8 \pm 07$ kJ mol^{-1}, is in a excellent agreement with the enthalpy magnitude observed previously [9–10] for many M_3LnX_6 compounds (M = Rb, Cs; Ln = lanthanide), ascribed to enthalpy of the solid-solid phase transition. Accordingly, the effect at 726 K can be attributed to a solid-solid phase transition in the Cs_3PrBr_6 compound.

An endothermic peak was observed in addition to liquidus and eutectic effects on the heating thermograms for samples with $PrBr_3$ molar fraction $0.548 < x < 1$ at 835 K. A Tamman diagram (effect related enthalpy vs. $PrBr_3$ molar fraction, Fig. 1e) gives $x = 0.674 \pm 0.009$, in good agreement with the theoretical value $x = 0.666$ for the $CsPr_2Br_7$ compound. Thus, the effect at 835 K can be attributed to a solid-solid phase transition in $CsPr_2Br_7$.

And finally an additional, very small endothermic effect of unknown origin (black circles in Fig. 2) was observable at about 862 K in all mixtures with molar fraction of praseodymium bromide $0.666 < x < 1$.

All the results of DSC investigation are presented in Table 1, and the complete phase diagram is shown in Figure 2.

Our finding for eutectic temperatures (850 K, 767 K, and 870 K) are in a good agreement with those given in literature [4] (848 K, 759 K, and 853 K, respectively). However, a significant difference was found for the melting temperature of Cs_3PrBr_6 and $CsPr_2Br_7$ compounds. We determined these temperatures as 1051 K and 896 K, respectively, whereas literature data are significantly lower (1032 K and 873 K, respectively). In addition we determined precisely the composition of eutectics, which was not given in literature [4].

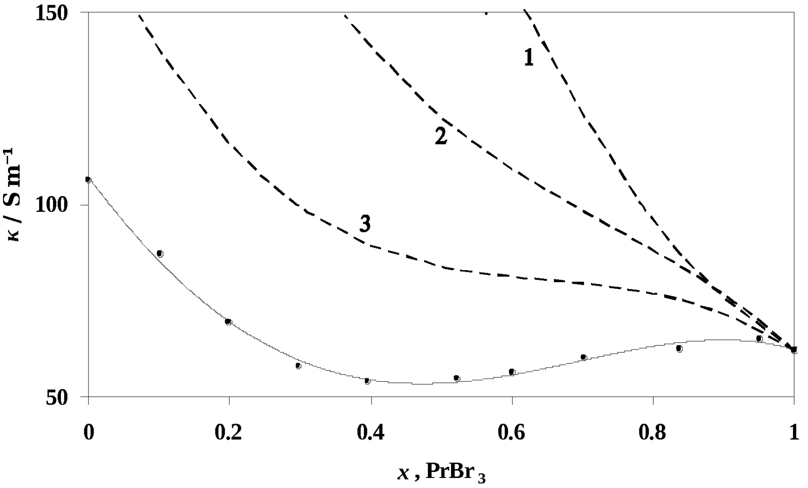

Fig. 3. Electrical conductivity isotherms of $PrBr_3$-MBr liquid mixtures at 1050 K; black circles and solid line: experimental results and polynomial fitting on CsBr system; broken lines: polynomial fitting of results on LiBr (1), NaBr (2), and KBr (3) systems.

Table 1. DSC results for $PrBr_3$-CsBr binary system.

x, $PrBr_3$	T / K Cs_3PrBr_6 phasae transition	T / K CsBr-Cs_3PrBr_6 eutectic	T / K Cs_3PrBr_6-$CsPr_2Br_7$ eutectic	T / K $CsPr_2Br_7$-$PrBr_3$ eutectic	T / K $CsPr_2Br_7$ transition	T / K liquidus
0.000	–	–	–	–	–	909
0.025	722	849	–	–	–	903
0.050	724	850	–	–	–	891
0.078	725	850	–	–	–	876
0.100	726	849	–	–	–	850
0.123	726	848	–	–	–	
0.149	727	849	–	–	–	938
0.173	729	851	–	–	–	983
0.198	729	851	–	–	–	1016
0.224	729	850	–	–	–	1039
0.250	726	–	–	–	–	1051
0.298	726	–	765	–	–	1026
0.352	725	–	767	–	–	951
0.401	725	–	768	–	–	868
0.450	724	–	768	–	–	767
0.505	724	–	767	–	–	813
0.541	724	–	768	–	–	837
0.601	720	–	767	–	834	879
0.666	–	–	–	–	835	896
0.674	–	–	–	868	835	898
0.698	–	–	–	869	835	893
0.721	–	–	–	870	835	888
0.739	–	–	–	872	835	879
0.790	–	–	–	869	835	889
0.842	–	–	–	869	836	932
0.898	–	–	–	870	836	941
0.950	–	–	–	870	836	958
1.000	–	–	–	–	–	960

3.2. Electrical Conductivity

The electrical conductivity of the $PrBr_3$-CsBr liquid mixtures was measured for the first time. Experimental determinations were conducted over the entire composition range in steps of about 10 mol%, and a wide temperature range.

The experimental conductivity κ data of the liquid phase were fitted to the second-order equation against temperature (T):

$$\ln(\kappa) = A_0 + A_1\left(\frac{1000}{T}\right) + A_2\left(\frac{1000}{T}\right)^2, \quad (1)$$

where A_0, A_1, and A_2 are coefficients determined by the least-squares method. The activation energy E_A, evaluated by analogy to the Arrhenius equation as

$$E_A(T) = -R\frac{d\ln(\kappa)}{d\left(\frac{1000}{T}\right)}, \quad (2)$$

where R is the gas constant, becomes

$$E_A = -R\left[a_1 + 2A_2\left(\frac{1000}{T}\right)\right]. \quad (3)$$

All A_i coefficients are listed in Table 2, together with the E_A values determined at 1050 K for all $PrBr_3$-CsBr mixtures.

The experimental conductivity isotherm at 1050 K was plotted against the mole fraction of $PrBr_3$ in Figure 3. For comparison isotherms for the analogous systems with LiBr, NaBr, and KBr [1,5] are also included (for the sake of clarity, the scale specific to the CsBr system was adopted, thus with a reduced view for other systems). The electrical conductivity decreases with increasing radius of the alkali metal cation, i. e. from lithium to cesium. The relative changes are significantly larger in the alkali bromide-rich region. In

Table 2. Coefficients of the equation $\ln\kappa = A_0 + A_1(1000/T) + A_2(1000/T)^2$ and the activation energy of the electrical conductivity E_A of liquid PrBr$_3$-CsBr binary mixtures (M = Rb, Cs) at 1050 K: κ in S m^{-1}, ln(s) is the standard deviation of ln κ, n the number of experimental data points.

x (PrBr$_3$)	Temp. range (K)	A_0 S m^{-1}	A_1 S m^{-1}K	A_2 S m^{-1}K^2	ln(s)	n	E_A at 1050 K (kJ/mol)
0.000	936 – 1137	4.9549	0.8146	−1.1708	0.0011	1073	11.594
0.101	985 – 1100	6.9296	−3.3755	0.8267	0.0043	287	14.973
0.199	985 – 1100	6.9526	−3.5264	0.7088	0.0041	277	18.094
0.298	1008 – 1100	7.1083	−4.2324	1.0821	0.0019	201	18.052
0.393	883 – 1100	4.4497	1.1133	−1.6752	0.0045	473	17.273
0.522	900 – 1100	4.1647	1.7061	−1.9682	0.0023	468	16.983
0.600	860 – 1100	3.4819	3.3011	−2.8597	0.0046	558	17.841
0.703	876 – 1100	3.0528	4.5695	−3.6481	0.0049	497	19.782
0.836	902 – 1100	3.6643	3.8220	−3.4943	0.0055	457	23.560
1.000	977 – 1170	4.9342	1.6942	−2.6688	0.0027	454	28.178

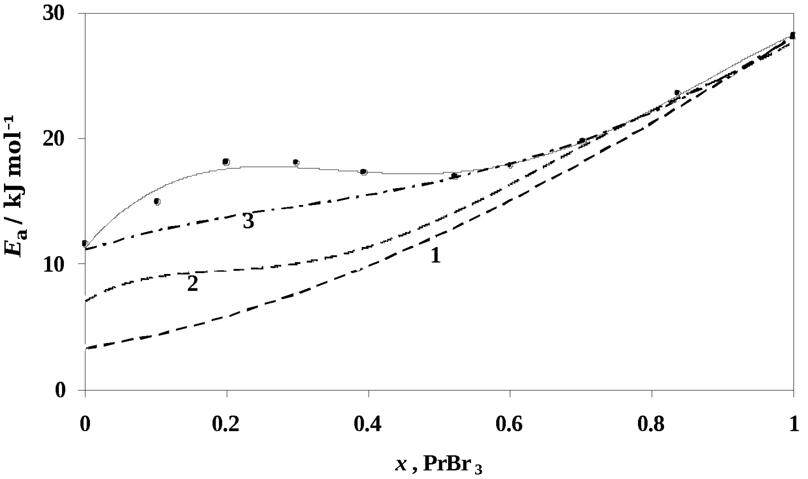

Fig. 4. Activation energy at 1050 K of PrBr$_3$-MBr liquid mixtures; black circles and solid line: experimental results and polynomial fitting on CsBr system; broken lines: polynomial fitting of results on LiBr (1), NaBr (2), and KBr (3) systems.

the praseodymium bromide-rich region the conductivity behaviour is somewhat more complicated. Its smooth decrease in the systems with LiBr and NaBr becomes smaller in the KBr system, and transforms into a broad minimum situated at $x \approx 0.4$ in the system with CsBr.

Figure 4 shows the activation energy at 1050 K as a function of composition. For comparison, activation energy data are also included for the analogous systems with LiBr and NaBr [1] and KBr [5]. Whereas in the system with LiBr the activation energy increases smoothly with PrBr$_3$ concentration, in the systems with heavier alkali bromides its behaviour is a little bit different. A stabilization effect of E_A, although somewhat unclear, seems to occur in the range of 25 – 50 mol% of PrBr$_3$ for the system with NaBr and KBr. In the system with CsBr the activation energy increases up to about 20 mol% of PrBr$_3$ and becomes stable up to about 60 mol% of PrBr$_3$. This plateau can be explained in terms of coexistence of different forms of complexes as evidences by Raman spectroscopy [11]. These investigations showed that octahedral LnBr$_6^{3-}$ ions are formed in LnBr$_3$-MBr liquid mixtures. These ions constitute the predominant species in the MBr-rich liquid mixtures. As the LnBr$_3$ concentration increases distorted octahedral species occurs, which are bridged by bromide anions.

Figure 4 clearly illustrates also that the activation energy increases with the alkali cationic radius particularly in the MBr-rich melts. It is likely that this is due to an increase of the PrBr$_6^{3-}$ complex concentration in the melt. The radius of the alkali metal cation will therefore govern the complex ion formation in the PrBr$_3$-MBr binary systems. Thus addition of CsBr to PrBr$_3$ favours complex ion formation more than LiBr, NaBr, or KBr, and results in a larger activation energy for electrical conductivity.

4. Conclusions

Two stoichiometric compounds, namely Cs_3PrBr_6 and $CsPr_2Br_7$, exist in the $PrBr_3$-CsBr binary system. Cs_3PrBr_6 undergoes a solid-solid phase transition at 726 K and melts congruently at 1051 K, whereas $CsPr_2Br_7$ undergoes a solid-solid phase transition at 835 K, and melts congruently at 896 K.

The specific electrical conductivity of $PrBr_3$-CsBr liquid mixtures is indicative of $PrBr_6^{3-}$ octahedral complexes formation in the melts.

Acknowledgements

Financial support by the Polish Ministry of Science and Higher Education from budget on science in 2007-2010 under the grant N N204 4098 33 is gratefully acknowledged.

L. R., M. B., and E. I.-S. wish to thank the Ecole Polytechnique de Marseille for hospitality and support during this work.

[1] E. Ingier-Stocka, L. Rycerz, M. Berkani, and M. Gaune-Escard, J. Molecular Liquids **148**, 40 (2009).
[2] H. J. Seifert, J. Therm. Anal. Cal. **7**, 789 (2002).
[3] H. J. Seifert, J. Thermal. Anal. Calor. **83**, 479 (2006), and references therein
[4] R. Blachnik and A. Jaeger-Kasper, Z. Anorg. Allg. Chem. **461**, 74 (1980).
[5] J. Rejek, L. Rycerz, E. Ingier-Stocka, and M. Gaune-Escard, J. Chem. Eng. Data **55**, 1871 (2010).
[6] J. Kutscher and A. Schneider, Z. Anorg. Allg. Chem. **408**, 135 (1974).
[7] Y. Fouque, M. Gaune-Escard, W. Szczepaniak, and A. Bogacz, J. Chim. Phys. **75**, 361 (1978).
[8] G. I. Janz, J. Phys. Chem. Ref. Data **2**, 17 (1988)
[9] L. Rycerz, High Temperature Characterization of LnX_3 and LnX_3-AX Solid and Liquid Systems (Ln = Lanthanide, A = Alkali, X = Halide): Thermodynamics and Electrical Conductivity, Ph.D. Thesis, Universite de Provence Aix-Marseille I, France, Marseille 2003.
[10] L. Rycerz, Thermochemistry of lanthanide halides and compounds formed in lanthanide halide-alkali metal halide systems (in Polish). Scientific Papers of Institute of Inorganic Chemistry and Metallurgy of Rare Elements; Series Monographs 35; Wroclaw University of Technology, Wroclaw 2004.
[11] G. M. Photiadis, B. Borresen, and G. N. Papatheodorou, J. Chem. Soc. Faraday Trans. **94**, 2605 (1998).